Thermal Performance Enhancement With DRX in 5G Millimeter Wave Communication System

AN HUANG[1], (Student Member, IEEE),
KUANG-HSUN LIN[1], (Graduate Student Member, IEEE),
AND HUNG-YU WEI[1,2], (Senior Member, IEEE)

[1]Graduate Institute of Communication Engineering, National Taiwan University, Taipei 10617, Taiwan
[2]Department of Electrical Engineering, National Taiwan University, Taipei 10617, Taiwan

Corresponding author: Hung-Yu Wei (hywei@ntu.edu.tw)

ABSTRACT The evolution of the communication and computation systems enables the user equipment (UE) to handle tremendous transmission data. However, the high-speed data processing also makes UEs release heat and might burn the chips inside the devices. The thermal issue would be more critical in millimeter-wave communications. The massive antenna arrays and the radio frequency modules not only drain the UE battery but also heat the devices. 3GPP also identified the thermal issue and suppressed heat generation by temporarily reducing UE capability in Release 15. In this work, instead of reducing the UE capability, we propose to apply the beam-aware Discontinuous Reception (DRX) mechanism to manage the power consumption and temperature of UEs simultaneously. We are the first to analyze the temperature for UEs with DRX configured. A semi-Markov model is provided, and we employ it to estimate the sleep ratio, packet delay, and steady temperature. We use a simulation program to verify the proposed analytical model. When comparing the beam-aware DRX with the baseline 5G NR DRX operation, we find that the beam-aware scheme reduces the steady temperature from $38.2°C$ to $26.7°C$. The results show that Beam-Aware DRX could solve the thermal issue without sacrificing much performance of packet delivery latency.

INDEX TERMS DRX, overheating, heat dissipation, thermal analysis, cross-layer design, serving beam pattern, 5G, beamforming, mmWave.

I. INTRODUCTION

Recently, the increasing number of connected user equipment (UE) causes the explosion of data traffic over the communication networks. To increase the throughput for the communication requirements in the fifth-generation (5G) New Radio (NR) networks, the network operators come up with one prospective solution, which is exploiting the unused spectrum with enormous available transmission resources, such as millimeter wave (mmWave) frequency bands [1]. Therefore, mmWave technology development is imperative for foreseeable communication networks, including beamforming technology [2]–[5].

Although the beamforming technology could enhance the directional links and increase the transmission rate in

The associate editor coordinating the review of this manuscript and approving it for publication was Chien-Fu Cheng.

mmWave bands, it brings a severe challenge in power as well [6], [7]. The power amplifier (PA) should be used at a higher voltage level than that of the fourth-generation (4G) Long Term Evolution (LTE) PA, enabling the mobile devices to satisfy the 5G communication requirements. When PA operates at a high voltage level, the saturated output power and gain limitation makes the power efficiency drop massively and generates a considerable amount of thermal energy [8]. Therefore, the massive antenna array used in mmWave beamforming technology consumes higher power than traditional devices' antennas modules. Besides, the compact size of the beamforming antenna generates more severe heat, which increases the temperature of devices [9], [10]. The circuit's power for a mmWave antenna is close to one of the processors in a smartphone [11]. If a UE turns on its RF module to receive the data for a continuous long time, the temperature could quickly achieve uncomfortable

temperature [12]. The overheating of mobile devices damages the function of devices and user experiences, especially for wearable devices [13].

Discontinuous Reception (DRX) is one of the most critical energy efficiency mechanisms on the UE side. Based on the DRX operations, a UE can control its radio-frequency (RF) module to decrease power consumption and confine packet delay. It is expected that UEs in 5G networks will continue using the DRX mechanism to save power [14]. In addition to power efficiency, DRX operations also have an enormous impact on mobile devices' heat. By controlling UEs' RF circuit, a DRX mechanism could reduce a considerable amount of heat from the mmWave antennas circuits. To the best of the authors' knowledge, there is no research focusing on the relationship between the DRX mechanism and the heat dissipation of UEs. Although it is intuitive to reduce the mobile devices' temperature with DRX mechanisms, how to determine the DRX parameter value for thermal performance enhancement and the amount of decreasing temperature when we change the DRX configuration are unclear. Thus, we would like to evaluate and analyze UEs' thermal performance under different DRX configurations.

Moreover, we found that a DRX mechanism with the beam-aware design, which was used to improve UEs' power efficiency in mmWave beamforming networks, further reduces the temperature easily [15]–[18]. Since the UEs' temperature increases massively when their RF modules are turned on for a continuous period [13], the discrete wake-up behavior in beam-aware design could maintain the low temperature. In the 5G mmWave communication systems with the beamforming technology, the gNB would choose some beams in each time-slot to serve the corresponding UEs sequentially. When the UEs' RF module is turned on only when the gNB serves the UEs, the UEs will not wake up for a continuous long time. As a result, the UEs could keep their temperature at a relatively low level.

In this paper, we explored the beneficial effect of the DRX mechanism on the temperature of UEs. Besides, with the awareness of both the overheating issue and the beam patterns in mmWave bands, a DRX mechanism with a beam-aware cross-layer design was proposed to reduce more heat than the NR baseline scheme. The main contributions of this work are summarized as follows.

- This work is the *first* research exploring UEs' thermal performance under a DRX operation. We evaluate UEs' temperatures under different DRX configurations and suggest a prospective direction for thermal enhancement designs. (§IV)
- We apply a beam-aware cross-layer design in [18] to reduce UEs' temperatures. According to the observation of a UE's thermal performance in §IV, the UE following a beam-aware behavior could prevent overheating problems effectively. (§V)
- The thermal analysis of UEs with a DRX mechanism is provided to evaluate the performance better. The

expected values of the main performance metrics, i.e., sleep ratio, packet delay, and steady temperature, are analyzed via a semi-Markov model. (§VI and §VII)

II. BACKGROUND

A. BEAMFORMING TECHNOLOGY IN mmWave COMMUNICATION

The mmWave communication technology enables future networks with a higher data rate, which meets the transmission requirements in 5G communication systems. However, the tremendous propagation loss and mmWave bands' directionality shorten the communication distance between gNBs and UEs. With beamforming technology, the gNB concentrates the transmission power in particular directions so that the received power of the UEs could be enhanced. Although beamforming technology is essential for the evolution of communication [2], [3], the antenna array with beamforming technology generates extreme heat power, which may damage the functionality of communication devices [9], [10]. With the assistance of robust cooling systems, the temperature of gNBs could decrease effectively. As for wireless mobile devices without external cooling systems, they are easy to encounter overheating problems. Therefore, the technology of reducing the temperature inside mobile devices is essential in future communication systems.

B. THE ISSUE OF OVERHEATING IN 3GPP STANDARDIZATION

As the UE capability improves in the 3GPP NR system, the manufacturers identified that the high computation and communication capabilities would make the UE overheated. Therefore, 3GPP started the related specification in 2017. To solve UE overheating, 3GPP proposed a procedure called UE assistance information [19]. This procedure enables the UEs to report their preferred configurations to the gNB when the UE is suffering from a high temperature. With the assistance information, the gNB could temporarily treat the UE as the one with reduced capabilities and reconfigure it. By reducing the number of component carriers, the bandwidth, and the MIMO layers, the UE could communicate at a lower transmission rate and cool down its radio frequency front end and its computation units [20].

C. DRX MECHANISM IN 3GPP STANDARD

The DRX mechanism proposed in the 3GPP standard is designed for UE power saving [21]. When a UE is configured with DRX, it goes to sleep when there is no data transmission and periodically wakes up to check if the downlink data indication exists every DRX cycle (see Figure 1). If the gNB transmitted new data, the UE stays active to receive the incoming data. After that, the UE starts dormancy again. During the dormancy period, the UE is allowed to turn off its radio frequency module and skip data transmission monitoring to save power.
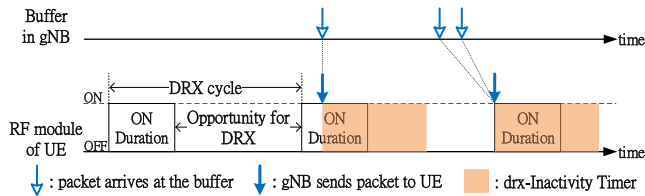
FIGURE 1. DRX mechanism in 3GPP standard [19]. There are an *ON Duration* and an *Opportunity for DRX* in one DRX cycle. Once a UE receives any packets, it resets its *drx-Inactivity Timer* and extends the *ON Duration* time. The gNB buffers the packets arriving in the *Opportunity for DRX* and retransmits them in the next *ON Duration*.

D. UE ASSISTANCE INFORMATION FOR DRX MECHANISM

After the UE assistance information standardization, 3GPP also proposed integrating the DRX configuration into the feedback information in release 16 [20]. When a UE has a different requirement level of power-saving and wants to change the current DRX setting, the UE could provide the preferred DRX configurations, such as the length of the DRX cycle and *drx-Inactivity Timer*, to the gNB. The gNB could then configure the UE properly to meet the requirement. Note that the gNB might not satisfy the UE because the reconfiguration of DRX for a UE might affect other UEs' DRX performance. Thus, an algorithm is still essential for the gNB to handle the reported assistance information.

III. RELATED WORK
A. LTE DRX

Until now, researchers have investigated power saving mechanisms in LTE cellular networks. Pocovi *et al.* found that DRX patterns and Scheduling Request significantly impact the possible latency and reliability in the LTE networks [22]. Considering the constraints on delay or power consumption, Ferng *et al.* proposed a DADRX-AP scheme enabling radio networks to find suitable parameter settings for UEs [23]. The Internet-of-Things (IoT) devices also encounter the problem of a massive amount of power consumption. Under IoT scenarios, adaptive DRX designs are proposed, and the packet delay and the sleep ratio of IoT devices are analyzed [24]–[27]. The development of energy harvesting is a potential method further to enhance IoT devices' power efficiency [28], [29].

B. 5G NR DRX

For the 5G NR network systems, the DRX mechanisms with the novel power-saving features are evaluated under various services [30]–[32]. Many researchers pay attention to the novel wake-up signal to save more power under DRX operation [33]–[37]. As for the 5G mmWave communication networks, mmWave radio is easy to be blocked by the buildings. Therefore, the studies of DRX mechanisms under dual connectivity scenarios are essential in the mmWave band communication [38], [39]. There is plenty of research focusing on the impact of beamforming on the DRX mechanism. The DRX mechanism's performance could be improved with

the awareness of the directional link in mmWave bands [15], [18]. Under different applications and service scenarios, the novel DRX design integrated with the process of beam searching is proposed and evaluated [40]–[46].

C. THERMAL MANAGEMENT

To reduce the thermal restriction, most researchers focus on the thermal management methods in mobile devices instead of the DRX mechanism integrated with the thermal design. The dynamic energy and thermal management (DTM) methods for multi-core mobile devices are provided in [47], including dynamic power management, dynamic voltage frequency scaling, and customization of processors adaptive to the application. Singla *et al.* presented a dynamic thermal and power management algorithm based on a reasonable temperature prediction [48]. With the predicted temperature, this algorithm could keep the processors operating within the permissible temperature. Considering the mobile gaming application, Praksah *et al.* proposed a control-theory based DTM that cooperatively scales both central and graphics processing units [49]. Most DTM would sacrifice the application performance to avoid thermal emergencies. Sahin and Coskun analyzed the impact of application duration and the temperature of existing DTM methods, then proposed a QoS-aware technique to improve the performance [50]. Another solution to cooling mobile electronic devices is using phase change material (PCM). While changing phase from solid to liquid, the PCM could effectively absorb the electronic components' dissipating heat [51].

D. THE DIFFERENCE BETWEEN THIS WORK AND PREVIOUS RESEARCH

Compared with the previous DRX research, we focus on UEs' thermal performance under different DRX configurations and different DRX schemes. The overheating issue is a pressing challenge for the UEs in 5G NR systems, especially with mmWave beamforming technology. Due to a lack of robust cooling systems, mobile devices are easy to malfunction with the massive amount of wasted heat. In addition to the power efficiency and the packet delay, we emphasize the UEs' thermal performance under DRX operation. To the authors' best knowledge, the thermal analysis for the steady temperature with DRX mechanisms is first provided in this research work. Besides, compared with the NR baseline scheme, we proposed that a DRX mechanism with a beam-aware design could reduce the steady temperature more effectively. The beam-aware DRX evaluated in this paper is the same as the Beam-Aware DRX in [18] without Dynamic-Configured Beam Frame. Therefore, the UEs only operate beam-aware DRX in Static-Configured Beam Frames.

IV. THERMAL PERFORMANCE OBSERVATION FOR NR BASELINE DRX

Via the UE assistance information, gNBs could reconfigure UEs' DRX parameters to decrease their temperature. Although DRX is served as one of the possible options to deal

with overheating problems, there is no research focusing on UEs' thermal performance under DRX operation. Therefore, we would like to evaluate UEs' temperature under different NR DRX configurations to investigate how to configure DRX parameters to reduce UEs' temperatures in the following. The packet arrival rate is set as $0.03\ ms^{-1}$, and the total number of beams is 8. Besides, the environmental temperature is $25°C$, and the highest temperature of the RF module is $45°C$.
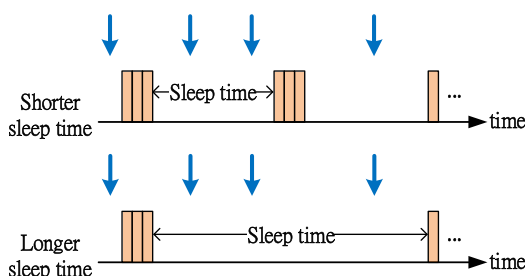
A. LONGER SLEEP TIME VS. SHORTER SLEEP TIME

To investigate the effect of DRX operation on the temperature and verify the theoretical analysis derived in §VII-C1, we use the different DRX parameter settings in the identical network scenarios. That is, we focus on the temperature of a UE with various DRX configurations. The network topology is the same, and the packet arrival rate is fixed to $0.03\ ms^{-1}$. In Figure 2, the UE is configured with different length of DRX cycles and the fixed *drx-Inactivity Timer*. The length of *drx-Inactivity Timer* is $40\ ms$, and that of DRX is 80 or $320\ ms$ as Figure 2(a) shows. With the fixed length of *drx-Inactivity Timer*, the longer the DRX cycle is, the longer the UEs' sleep time is. The RF module is turned off when the UE goes to

sleep, so the longer DRX cycles lead to a more extended cooling period. Therefore, after the same simulation time, the UE with longer DRX cycles could lower its temperature than the UE with a shorter DRX cycle in Figure 2(b).

B. LONGER ON DURATION VS. SHORTER ON DURATION UNDER THE SAME TIMER RATIO

Figure 3 demonstrates the UE's temperature under DRX operations when the UE is configured with the short *ON Duration* configuration and the long *ON Duration* configuration. These two settings are illustrated in Figure 3(a). In the former one, the DRX cycle length is $10\ ms$, and the length of *drx-Inactivity Timer* is $2\ ms$. As for the latter one, the length of the DRX cycle and one of *drx-Inactivity Timer* are set to $100\ ms$ and $20\ ms$. Therefore, we could explore the effect of different DRX cycle lengths on the temperature under the same timer ratios. That is, the ratio of the length of *drx-Inactivity Timer* to that of DRX cycles are identical, but the DRX cycle lengths are different in these two configurations. In Figure 3(b), the UE with the short *ON Duration* configuration decreases more temperature than the UE with the long *ON Duration*
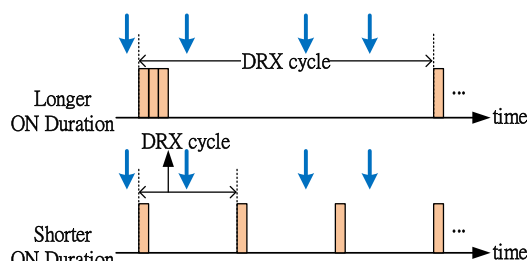
(a) An illustrative example of the two different DRX settings. The length of *drx-Inactivity Timer* is fixed to $40\ ms$ in both settings. For the shorter and the longer sleep time configurations, we set the length of the DRX cycle to $80\ ms$ and $320\ ms$, respectively.
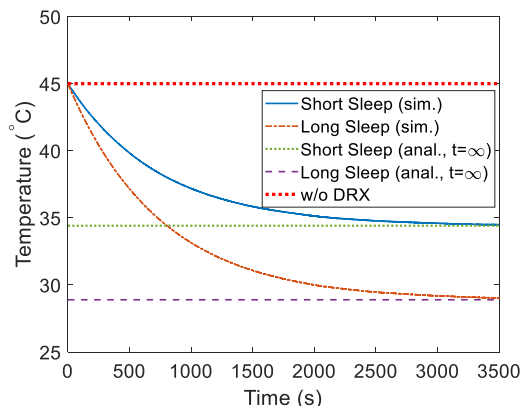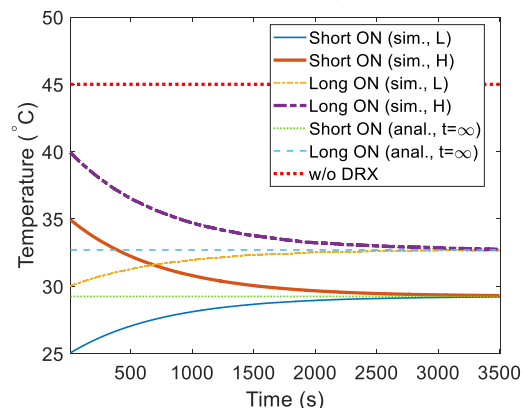
(b) The simulated and analytical thermal performance of the two different DRX configurations. We verify the results by the analytical model for steady temperature in §VII-C1. The theoretical results fit the UE's temperature in the long term.

FIGURE 2. An initial temperature evaluation of NR DRX. The result shows that the UE with long sleep time could reduce a massive amount of temperature.

(a) An illustrative example of the two different DRX settings. For the short ON Duration configuration, we set the length of *drx-Inactivity Timer* and the DRX cycle as $2\ ms$ and $10\ ms$. For the long ON Duration setting, the length of *drx-Inactivity Timer* is $20\ ms$, and that of the DRX cycle is $100\ ms$.

(b) The simulated and analytical thermal performance of the two different DRX configurations, where H presents the initial temperature is high, and L presents that is low. We verify the results by the analytical model for steady temperature in §VII-C1. The theoretical results fit the UE's temperature in the long term.

FIGURE 3. An initial temperature evaluation of NR DRX. The result shows that the UE could reduce the temperature if it wakes up frequently, and the RF module is only turned on for a short time.
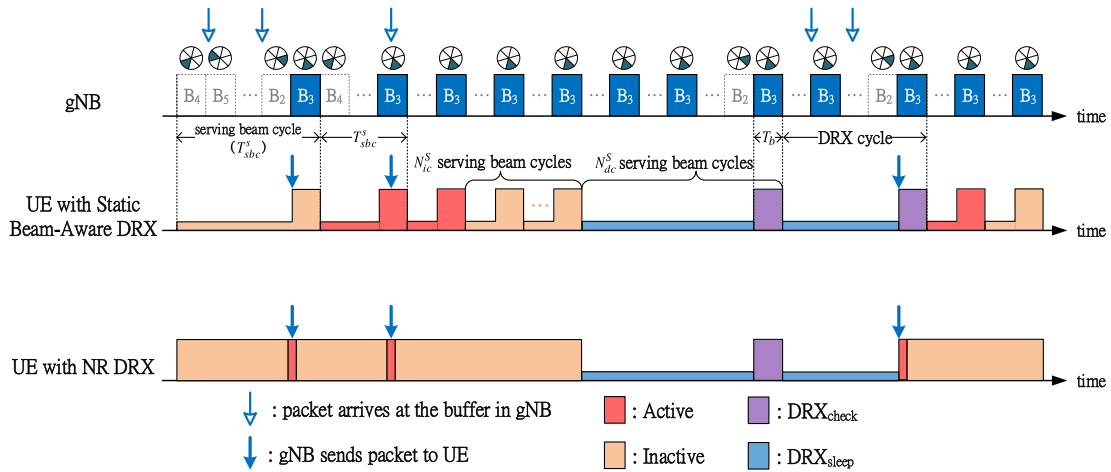
FIGURE 4. The beam-aware DRX operation in the static serving beam cycles. Based on the serving beam cycle, the UE on Beam-3 only monitor PDCCH when the gNB uses Beam-3 to schedule data; however, the RF module of the UE with NR DRX would be turned on continuously. In *Active* and *Inactive*, the UE wake-up pattern follows the serving beam cycles. Any packet arrivals extend the active time of the UE. After the long sleep time (DRX_{sleep}), the UE's RF module is turned on for a short time (DRX_{check}). If there are any incoming packets, the UE will return to *Active*.

configuration. In other words, the UEs waking up for a short time frequently reduce the temperature effectively. Therefore, the DRX mechanism with a beam-aware design could further enhance the thermal performance of UEs. Under a beam-aware DRX operation, the UE's RF module is turned on only for a short beam period many times rather than for a continuous long time. As a result, a beam-aware DRX could keep the UEs' temperature low even if the traffic load is heavy.

V. THERMAL ENHANCEMENT WITH BEAM-AWARE DESIGN

UE overheating is a critical problem for the NR system, especially in mmWave communication with beamforming technology. 3GPP enabled UEs to feedback assistance information so that the gNB could relieve the loading of overheated UEs. However, instead of reducing the capabilities of overheated UEs, we proposed to solve the problem of UE overheating by the configuration of the DRX mechanism. Although the DRX mechanism is designed for UE power saving in the 3GPP standard, it is evident that the UE temperature would decrease during the dormancy period. Moreover, the UE can also report the DRX assistance information in the 3GPP standard of release 16. However, there is a lack of studies investigating the relationship between UEs' DRX behaviors, and UEs' temperature. Consequently, we focus on the thermal analysis of the DRX mechanism in this work. In §IV, we compare the thermal performance of UEs under different DRX configuration. The results in Figure 2 show that the longer sleep time could reduce the UE's temperature with the same length of *drx-Inactivity Timer*. Moreover, when the DRX timer ratios are identical in Figure 3, the UE configured with the shorter DRX cycle and the shorter *drx-Inactivity Timer* could decrease its temperature massively. A beam-aware design in [18] makes a UE wake up for a short

time frequently, and the UE's behavior is similar to that with the shorter *ON Duration* configuration in Figure 3(a). Therefore, according to the initial observation of the temperature under NR DRX operation, we propose to employ the DRX with a beam-aware design to reduce the increasing amount of temperature of UEs.

Beam-Aware DRX design is proposed in our previous work [18] to improve DRX energy efficiency. Here, we further extend the beam-aware DRX design to improve the thermal performance of wireless devices. According to our observation in §IV, we find that the UEs could reduce their temperature with frequent and short wake-up behaviors. Therefore, we avoid using the Dynamic-Configured Beam Frame in [18] to prevent UEs from waking up for an extended time period under heavy traffic load. In this paper, the UE operates the beam-aware DRX mechanism in the Static-Configured Beam Frames as Figure 4 shows. That is, the gNB would use only one beam to schedule data in each time-slot. Via the beam management process [52], the gNB would find out the best beam pair for each UE. It sequentially serves each UE with the beam pointing to every direction in one serving beam cycle (T_{sbc}^s). According to the repeated serving beam cycles and the beam pair information, the gNB could configure UEs with suitable DRX parameter settings. And then, the UE wakes up only when the gNB uses the corresponding beam to serve itself. Therefore, the beam-aware design could prevent UEs from wasting power to wake up when the gNB is scheduling data to another UE. In *Active* and *Inactive*, the UE with the beam-aware DRX would wake up for one beam period (T_b) in each serving beam cycle to monitor PDCCH. Similar to the NR DRX, any packet arrivals would extend the UE's active time under the beam-aware DRX operations. When the UE does not receive any packets for a predefined period, the UE will enter DRX_{sleep}, i.e., a long sleeping time to decrease its temperature. The gNB buffers all

packets when the UE is sleeping. After a long sleeping time, the UE enters DRX_{check} to wake up for a short time, and the gNB could retransmit the buffered packets to it. Then, the UE would return to *Active*.

VI. THE SEMI-MARKOV CHAIN DRX MODEL

In this paper, the beam-aware DRX operation applies the Static-Configured Beam Frames for better thermal performance. Similar to the mathematical model in [18], the DRX mechanism includes four states in Figure 4: *Active*, *Inactive*, DRX_{check}, and DRX_{sleep}. Nevertheless, since we do not apply Dynamic-Configured Beam Frames in this paper, the state transitions between different states are revised to model the static beam patterns. The differences in modeling are described in the following three aspects.

1) Instead of buffered packets, any packet arriving at UEs in *Active* would make them stay in *Active*.
2) If there is no packet arriving in the UE with the last *Inactive*, the UE enters DRX_{sleep} rather than DRX_{check}.
3) After leaving DRX_{sleep}, the UE would only enter DRX_{check} in the beam-aware DRX in this paper.

With the semi-Markov model in Figure 5, we could model the beam-aware DRX operation in Figure 4. The gNB could use one beam to schedule the UEs in each time-slot and sequentially serves the UEs on the beams of all directions in one serving beam cycle. With the beam-aware DRX mechanism, the destination UE turns on its RF module only when the gNB uses the corresponding beam to serves. In contrast, when the gNB serves other UEs on the different beams, the destination UE goes to sleep. Therefore, the UEs could reduce the temperature in *Active* and *Inactive* effectively. There are one DRX_{check} and one DRX_{sleep} in a DRX cycle. We describe these four states in the following.

1) *Active* (S^S1): The UE staying in *Active* turns on its RF module to monitor downlink signal, transmit data, and receive packets. The beam-aware DRX operation is different from the UE behavior in 5G NR DRX, which is turning on its RF module all the time to receive data. Instead, the UE turns on its radio only when the gNB serves it for a beam period in each serving beam cycle. If any packets arrive at the UE, the UE stays in its current state at the end of this state; otherwise, it enters *Inactive*.

2) *Inactive* (S^S2_m, $\forall m \in \{1, 2, \ldots, N_{ic}^S\}$): Figure 5 illustrates that there are N_{ic}^S substates in *Inactive*. The UE behavior in each substate of *Inactive* is the same as the one in *Active*. Similarly, the duration of a substate is fixed to one serving beam cycle (T_{sbc}^s). *Inactive* in the beam-aware DRX is similar to the *drx-Inactivity Timer* in the beam-aware DRX mechanism, and the total number of substates (N_{ic}^S) corresponds to the timer length. Thus, any packets arriving at the UE could move it to *Active* and reset the timer. Otherwise, the timer will count downs, so the UE enters the next substate in *Inactive* or DRX_{sleep} with no packets arriving.

3) DRX_{check} (S^S3): In Figure 4, a DRX_{sleep} and a DRX_{check} construct a DRX cycle. In DRX_{check}, the UE wakes up for one beam period (T_b) to monitor downlink signal. If there are any packets arriving in DRX_{sleep} and buffered, the gNB would retransmit them after the UE enter DRX_{check}. Therefore, the UE could receive the buffered packets. The DRX cycle length is a multiple of T_{sbc}^s, so gNB would use the correct beam to serve the destination UE for a beam period at the end of DRX cycle. If any packets arrive at the UE in DRX_{sleep} or DRX_{check}, it would receive data at the end of the DRX cycle and enters *Active* in the next state; otherwise, it moves back to DRX_{sleep}.

4) DRX_{sleep} (S^S4): The UE turns off its RF module for $N_{dc}^S \cdot T_{sbc}^s - T_b$ in DRX_{sleep} to save power. No matter if there are packets or not, the UE will enter DRX_{check} after leaving DRX_{sleep}. The gNB would buffer the packets arriving in this state and retransmit them after the UE enters DRX_{check}.

VII. MATHEMATICAL FORMULATION

In this section, we would like to derive the thermal performance metric, i.e., steady temperature, under both the beam-aware and NR DRX operations. First, we use the semi-Markov Chain model in Figure 5 to model the transitions between different DRX operation states in §VII-A. Second, the UEs' temperatures could be obtained with the heating function and the cooling function in §VII-B. In §VII-C, we calculate the UEs' temperatures under the DRX operations with the semi-Markov Chain model, the temperature heating function, and the cooling function to solve the steady temperature.

In the analytical model, there are a gNB with N beams and several UEs randomly distributed in the cell. Figure 4 depicts that the gNB chooses one beam to schedule data for the UEs in each beam period (T_b) and serves UEs on beams pointing to all directions sequentially in one cycle. For each UE, the gNB serves it once every serving beam cycle ($T_{sbc}^s = N \cdot T_b$), and the serving time is one beam period (T_b). Thus, the DRX operation of each UE is the same. In the following, we will derive a steady temperature for
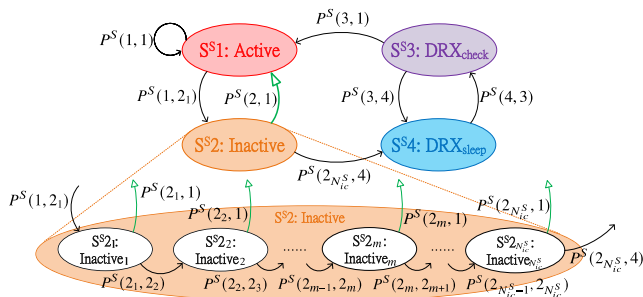

FIGURE 5. The semi-Markov model of each UE with the beam-aware DRX mechanism, where $P^S(2, 1) = \sum_{m=1}^{N_{ic}^S} P^S(2_m, 1)$.

each UE. The detailed derivation process of the traditional DRX performance metrics, including sleep ratio and packet delay, is in Appendix A. We use the Poisson process with parameter λ to model the packet arrival process, and the random variable of packet inter-arrival time is referred to as t_a. Besides, every UE is perfectly synchronized with the gNB. Since the transmission rate is exceptionally high in the mmWave band, we ignore the packet transmission time in this paper. In the following, the important notation used in the derivation is listed in Table 1.

A. TRANSITION PROBABILITY

We analyze the beam-aware DRX based on the semi-Markov model in Figure 5. To calculate the performance metrics of

TABLE 1. Notation list.

Symbols	The meaning of the symbol
N	Total beam number of one gNB
λ	Inter-arrival rate of UE
t_a	Inter-arrival time of UE
T_b	The length of one beam period
T_{sbc}^s	The length of one serving beam cycle
K_{env}	The environmental temperature
K_{RF}	The highest temperature of the RF module
τ	The time constant in thermal model
ΔK	The increasing temperature after a DRX cycle
$\mathcal{S}^S$	The set of every states in the beam-aware DRX
$P^S(m,n)$	The transition probability from state $S^S m$ to state $S^S n$, where $m, n \in \mathcal{S}^S$
$\Pi^S(m)$	The steady state probability in state $S^S m$, where $m \in \mathcal{S}^S$
N_{ic}^S	The total number of substates in Inactive
N_{dc}^S	The total number of serving beam cycle in one beam-aware DRX cycle
$T_h^S(m)$	The holding time of UE in state $S^S m$, where $m \in \mathcal{S}^S$
d_{act}^S	The delay of packet sent to UE in *Active* or *Inactive*
d_{sleep}^S	The delay of packet arriving in a beam-aware DRX cycle
$K_{H,m}^S$	The temperature at the end of the mth wake-up time in each beam-aware DRX cycle
$K_{L,m}^S$	The temperature at the end of the mth sleep time in each beam-aware DRX cycle
ΔK^S	The increasing temperature after a beam-aware DRX cycle
R^S	The sleep ratio of UE with the beam-aware DRX
D^S	The delay of packet sent to UE with the beam-aware DRX
K_∞^S	The steady temperature of UE with the beam-aware DRX
T_{check}^N	The length of *ON Duration* Timer if there is no packet arrival in NR DRX
T_I^N	The length of *drx-Inactivity Timer* in NR DRX
T_{sleep}^N	The length of the sleep time in a NR DRX cycle
K_H^N	The temperature at the end of the wake-up time in each NR DRX cycle
K_L^N	The temperature at the end of the sleep time in each NR DRX cycle
ΔK^N	The increasing temperature after a NR DRX cycle
K_∞^N	The steady temperature of UE in NR DRX

beam-aware DRX, we have to derive the transition probability firstly. The transition probability from state $S^S m$ to state $S^S n$ is denoted as $P^S(m, n)$, where $m, n \in \mathcal{S}^S$ and the state set of beam-aware DRX $\mathcal{S}^S = \{1, 3, 4\} \cup \{2_1, 2_2, \ldots, 2_{N_{ic}^S}\}$. We derive the state transition probabilities according to each state as follows.

1) **Transition probability from *Active*:** At the end of *Active*, the UE remains in the same state when there are any packet arrivals in T_{sbc}^s; otherwise, the UE enters *Inactive*. Therefore, the state transition is different from that in Beam-Aware DRX, which stays in *Active* when there are any buffered packets in the gNB [18]. The transition probabilities from *Active* to *Active* and *Inactive* are

$$P^S(1, 1) = \mathsf{Pr}\{t_a < T_{sbc}^s\} = 1 - e^{-\lambda T_{sbc}^s} \quad (1a)$$

$$P^S(1, 2_1) = 1 - P^S(1, 1) = e^{-\lambda T_{sbc}^s}. \quad (1b)$$

2) **Transition probability from *Inactive*:** Similar to *Active*, if the UE receive no packets in *Inactive*, it stays in *Inactive* or enters *DRX*$_{sleep}$ at the end of this state. Once receiving any packet arrivals, the UE moves to *Active* at the next state. It is worth noting that the UE with Beam-Aware DRX is moved to *DRX*$_{check}$ rather than *DRX*$_{sleep}$ if there is no packet arrival in the last *Inactive* substate [18]. The length of each substate in *Inactive* is T_{sbc}^s. For $m \in \{1, 2, \ldots, N_{ic}^S - 1\}$,

$$P^S(2_m, 1) = P^S(2_{N_{ic}^S}, 1) == 1 - e^{-\lambda T_{sbc}^s} \quad (2a)$$

$$P^S(2_m, 2_{m+1}) = P^S(2_{N_{ic}^S}, 3) = e^{-\lambda T_{sbc}^s}. \quad (2b)$$

3) **Transition probability from *DRX*$_{check}$:** The packets arriving *DRX*$_{check}$ and *DRX*$_{sleep}$ let the UE move to *Active* at the end of *DRX*$_{check}$. The UE will enter *DRX*$_{sleep}$ when no packets arrive at the UE. The transition probabilities from *DRX*$_{check}$ to *Active* and *DRX*$_{sleep}$ are

$$P^S(3, 1) = \mathsf{Pr}\{t_a < N_{dc}^S T_{sbc}^s\} = 1 - e^{-\lambda N_{dc}^S T_{sbc}^s} \quad (3a)$$

$$P^S(3, 4) = 1 - P^S(3, 1) = e^{-\lambda N_{dc}^S T_{sbc}^s}. \quad (3b)$$

4) **Transition probability from *DRX*$_{sleep}$:** At the end of *DRX*$_{sleep}$, the UE will enter *DRX*$_{check}$ whether there are any packet arrivals or not. Thus, the probability of entering *DRX*$_{sleep}$ is

$$P^S(4, 3) = 1. \quad (4)$$

As for Beam-Aware DRX, the UE may enter *DRX*$_{check}$ or *Active* depending on whether there are any buffered packets or not. The transition probabilities in this paper and that in [18] are different as well.

Therefore, the transition probability matrix of the beam-aware DRX is in Equation (5), as shown at the bottom of the next page.

B. THERMAL MODEL

We use the statement of Newton's Law of cooling in [53] to present the heat transfer in the UE when its RF module is turned on and turned off. The statement is

$$Q = h \cdot A \cdot (K(t) - K_{sur}), \tag{6}$$

where Q is the heat transfer rate, h is the heat transfer coefficient, A is the heat transfer surface area, $K(t)$ is the UE's temperature at time t, and K_{sur} is the surrounding temperature. With Equation (6), we could express $K(t)$ as

$$K(t) = K_{sur} + (K(0) - K_{sur})e^{-t/\tau}, \tag{7}$$

where τ is the time constant related to the material of UE. When the RF module of UE is turned on, the temperature of UE increases and reaches a maximal value (K_{RF}) after a long time. Besides, the UE's temperature decreases when the RF module of UE is turned off. The temperature of UE achieves the environmental temperature (K_{env}) if the cooling time is long enough. Therefore, we could use the following two functions to represent the UE's temperature when the RF module of UE is turned on and turned off. The heating function and the cooling function are

$$f_{ht}(K(t), t_{on}) = K_{RF} + (K(t) - K_{RF})e^{-t_{on}/\tau} \tag{8}$$

and

$$f_{cl}(K(t), t_{off}) = K_{env} + (K(t) - K_{env})e^{-t_{off}/\tau}, \tag{9}$$

respectively, where t_{on} and t_{off} are the wake-up time and the sleep time of UE.

C. STEADY TEMPERATURE

Steady temperature (K_∞) is the average temperature of UEs in the long term. When the temperature of UEs reaches a steady temperature, the expected increasing temperature ($E\{\Delta K\}$) after a DRX cycle should be zero. The range of the steady temperature is between the environmental temperature (K_{env}) to the highest temperature of the RF module (K_{RF}). For $K_{env} \le K_\infty \le K_{RF}$, we would like to find the value of the steady temperature (K_∞) via the following equation

$$E\{\Delta K(K_\infty)\} = \sum_k \Pr\{K_{end} = k\} \cdot \Delta K(K_\infty, k) = 0, \tag{10}$$
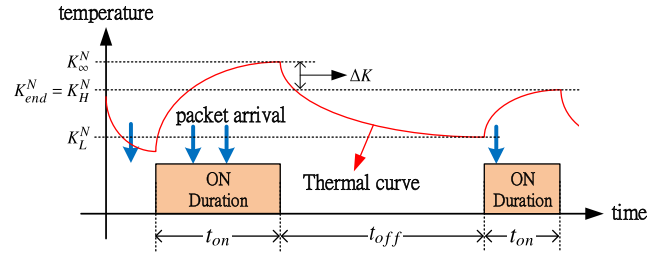

FIGURE 6. A toy example for the change in temperature of the UE with NR DRX mechanism in a DRX cycle. When the UE's RF module is turned off, the temperature decreases to the value K_L^N. The temperature increases up to the value K_H^N if the RF module is turned on. The length of wake-up time (t_{on}) and that of sleep time (t_{off}) affect the increasing temperature ($\Delta K = K_\infty^N - K_{end}^N$).

where K_{end} is the temperature of UEs at the end of a DRX cycle. Besides, the increasing temperature is expressed as

$$\Delta K(K_\infty, K_{end}) = K_{end} - K_\infty. \tag{11}$$

Figure 6 shows the toy example for the temperature of a UE with NR DRX. The UEs' temperature is changed based on the length of *ON Duration* (t_{on}) and the length of sleep time (t_{off}) in each DRX cycle. Since the length of sleep time in a DRX cycle is fixed in this paper, we need to derive the length of *ON Duration* to calculate the increasing temperature. The length of *ON Duration* is varied with the packet arrival time. If the length of *ON Duration* is long, the increasing temperature after a DRX cycle is positive; otherwise, the increasing temperature after a DRX cycle is negative. Besides, in the beam-Aware DRX, the number of each UE wake-up times in one DRX cycle also affects the increasing temperature. Therefore, to calculate the increasing temperature (ΔK), we need to derive the temperature at the end of a DRX cycle (K_{end}) according to the DRX mechanism.

To the best of our knowledge, no other researchers have analyzed the steady temperature of UEs with the NR DRX mechanism before. Thus, we will derive the steady temperature of the NR DRX (K_∞^N) as the baseline scheme and that of the beam-aware DRX (K_∞^S) in §VII-C1 and §VII-C2 respectively. Besides, to simplify the following deviations, we see the long sleep time as the first part and the *ON Duration* as the second part in a DRX cycle.

$$\mathbf{P^S} = \begin{bmatrix} P^S(1,1) & P^S(1,2_1) & 0 & 0 & 0 & 0 & \dots & 0 \\ P^S(2_1,1) & 0 & P^S(2_1,2_2) & 0 & 0 & 0 & \dots & 0 \\ \vdots & & & \ddots & & & & \vdots \\ P^S(2_m,1) & 0 & \dots & 0 & P^S(2_m,2_{m+1}) & 0 & \dots & 0 \\ \vdots & & & & & \ddots & & \vdots \\ P^S(2_{N_{ic}^B},1) & 0 & 0 & 0 & \dots & 0 & 0 & P^S(2_{N_{ic}^B},4) \\ P^S(3,1) & 0 & 0 & 0 & 0 & \dots & 0 & P^S(3,4) \\ 0 & 0 & 0 & 0 & \dots & 0 & P^S(4,3) & 0 \end{bmatrix} \tag{5}$$

1) THERMAL ANALYSIS MODEL OF NR DRX

Figure 6 shows that a DRX cycle contains one long sleep time (t_{off}) and one wake-up time (t_{on}) in NR DRX. Since the sleep time is fixed to T_{sleep}^N, we could use the heating function in Equation (8) and the cooling function in Equation (9) to express the temperature at the end of a DRX cycle as

$$K_{end}^N(K_\infty^N, t_{on}) = K_H^N = f_{ht}(K_L^N(K_\infty^N), t_{on}) \quad (12)$$
$$K_L^N(K_\infty^N) = f_{cl}(K_\infty^N, T_{sleep}^N), \quad (13)$$

where K_H^N is the UE's temperature after wake-up time and K_L^N is the UE's temperature after sleep time. For readability, we present the increasing temperature in NR DRX as

$$\Delta K^N(K_\infty^N, t_{on}) = \Delta K(K_\infty^N, K_{end}^N(K_\infty^N, t_{on})). \quad (14)$$

We need to derive the length of *ON Duration* (t_{on}), which affects the increasing temperature (ΔK^N). The *ON Duration* is extended when the UE receives any packets arriving in the *ON Duration*. As for the packets arriving in the UE's sleep time, they are buffered temporarily and transmitted after the UE wakes up. According to the packets arriving time, we could classify the events with different lengths of *ON Duration* into three cases in Figure 7. For each case, we derive the length of *ON Duration* and the probability of the corresponding event. In reality, the unit of the timer in NR DRX is time-slot. When the UE with NR DRX receives a packet, the *drx-Inactivity Timer* is reset at the end of the current time-slot, and the *ON Duration* is extended for T_I^N time-slots. If there is no packet in the DRX cycle, the UE will wake up for T_{check}^N and go to sleep for T_{sleep}^N.

- Case 1: If any packets arrive in the sleep time (T_{sleep}^N), the gNB buffers and retransmits them when the UE wakes up. Therefore, both the buffered packets arriving in the sleep time and ones arriving in the *ON Duration* would extend the *ON Duration*. In this case, if the length of extended *ON Duration* is $nT_b + T_I^N$, the probability of this event is $\Pr\{t_a < T_{sleep}^N\} \cdot P_{ext,n}^N$. $P_{ext,n}^N$ is the probability of the *ON Duration* extended n more time-slots once the *drx-Inactivity Timer* is reset. We could express $P_{ext,n}^N$ as Equation (15) shows.
- Case 2: When there is no packet arriving at the UE's sleep time, the UE will wake up for a short time (T_{check}^N) to check the packet arrivals. If there are any packets
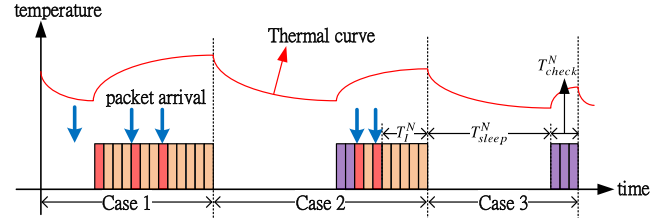
arriving in T_{check}^N, the *drx-Inactivity Timer* will be reset, and then the *ON Duration* is extended. We consider these three conditions:

1) There is no packet arrival in the sleep time,
2) A packet arriving at the UE at the mth time-slots in T_{check}^N,
3) The *ON Duration* is extended n more time-slots after *drx-Inactivity Timer* is reset.

If the mentioned conditions are satisfied, the length of the extended *ON Duration* should be $(m + n)T_b + T_I^N$. Besides, the probability of this event happening is $\Pr\{t_a \geq T_{sleep}^N\} \cdot e^{-\lambda T_b(m-1)}(1 - e^{-\lambda T_b}) \cdot P_{ext,n}^N$.

- Case 3: If there is no packet arrival in both the sleep time and the *ON Duration*, the UE's RF module is only turned on for a short time (T_{check}^N). Therefore, the *ON Duration* is T_{check}^N, and the probability is $\Pr\{t_a \geq T_{sleep}^N + T_{check}^N\}$.

Considering the mentioned three cases, we could express Equation (10) in NR DRX as Equation (16) shows.

2) THERMAL ANALYSIS MODEL OF THE BEAM-AWARE DRX

For the beam-aware DRX, each UE's RF module is turned on only when the gNB serves it, so the wake-up time (t_{on}) is fixed to T_b. There are many wake-up time intervals and sleep time intervals in a DRX cycle, so we use $K_{H,n}^S$ and $K_{L,n}^S$ to present the UE's temperature at the end of the nth wake-up time and that after the nth sleep time, respectively. In Figure 8, the temperature at the end of a DRX cycle is that at the end of the last wake-up time. Considering the total number of the wake-up times (n_{on}) in a DRX cycle, we could express the

FIGURE 7. The length of *ON Duration* affects the changing temperature of the UE with NR DRX. According to the packet arrival time, we divide the DRX operation with the different length of *ON Duration* into the following three cases: 1) packets buffered in the sleep time, 2) packets arriving after the UE wakes up, 3) no packet arriving.

$$P_{ext,n}^N = \begin{cases} e^{-\lambda T_I^N}, & \text{when } n = 0 \\ \sum_{s=1}^{\min\{n, T_I^N/T_b\}} e^{-\lambda T_b(s-1)}(1 - e^{-\lambda T_b})P_{ext,n-s}^N, & \text{otherwise} \end{cases} \quad (15)$$

$$\mathsf{E}\{\Delta K^N(K_\infty^N)\} = \Pr\{t_a < T_{sleep}^N\} \sum_{n=0}^{\infty} \Delta K^N(K_\infty^N, nT_b + T_I^N) \cdot P_{ext,n}^N$$

$$+ \Pr\{t_a \geq T_{sleep}^N\} \sum_{m=1}^{T_{check}^N/T_b} \sum_{n=0}^{\infty} \Delta K^N(K_\infty^N, (m+n)T_b + T_I^N)e^{-\lambda T_b(m-1)}(1 - e^{-\lambda T_b})P_{ext,n}^N$$

$$+ \Pr\{t_a \geq T_{sleep}^N + T_{check}^N\} \cdot \Delta K^N(K_\infty^N, T_{check}^N) = 0 \quad (16)$$
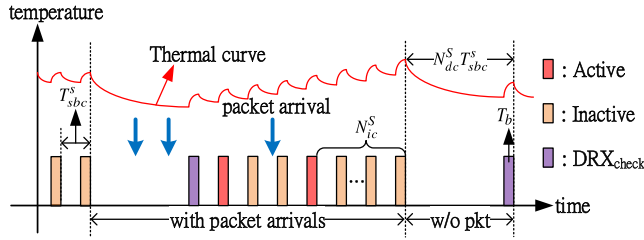
FIGURE 8. The change in temperature of the UE with the beam-aware DRX. When packets are arriving in *DRX$_{sleep}$* or *DRX$_{check}$*, the UE will enter *Active*, and its RF module will be turned on many times. Thus, the temperature increases after a DRX cycle. If there is no packet arrival, the UE wakes up once, and the temperature decreases.

temperature at the end of a DRX cycle as

$$K_{end}^S(K_\infty^S, n_{on}) = K_{H,n_{on}}^S, \qquad (17)$$

where

$$K_{H,n}^S = f_{ht}(K_{L,n}^S(K_\infty^S), T_b) \qquad (18)$$

$$K_{L,n}^S(K_\infty^S) = \begin{cases} f_{cl}(K_\infty^S, N_{dc}^S T_{sbc}^s - T_b), & \text{when } n = 1 \\ f_{cl}(K_{H,n-1}^S, T_{sbc}^s - T_b), & \text{otherwise} \end{cases} \qquad (19)$$

for all $n \in \{1, 2, \ldots, n_{on}\}$. For the readability, we present the increasing temperature in the beam-aware DRX as

$$\Delta K^S(K_\infty^S, n_{on}) = \Delta K(K_\infty^S, K_{end}^S(K_\infty^S, n_{on})). \qquad (20)$$

As Figure 8 shows, the UE enters *Active* after leaving *DRX$_{check}$* when there are any packets arriving at the UE in a DRX cycle. The total number of wake-up times (n_{on}) of the UE increases as well. If the number of UEs wake-up times increases to $n + N_{ic}^S + 2$ in a DRX cycle, the probability of this event should be $P^S(3, 1) \cdot P_{ext,n}^S$ where $P_{ext,n}^S$ is the probability of the UE waking up n more times once the UE enters *Active*. $P_{ext,n}^S$ is derived as Equation (21), as shown at the bottom of the page.

When there is no packet arrival in a DRX cycle, the UE wakes up once. The probability of no packet arriving at the UE is $P^S(3, 4)$. Therefore, in the beam-aware DRX, Equation (10) is

$$\mathsf{E}\{\Delta K^S(K_\infty^S)\}$$

$$= P^S(3, 1) \sum_{n=0}^\infty \Delta K^S(K_\infty^S, n + N_{ic}^S + 2) \cdot P_{ext,n}^S$$

$$+ P^S(3, 4) \cdot \Delta K^S(K_\infty^S, 1) = 0 \qquad (22)$$

VIII. NUMERICAL ANALYSIS AND SIMULATION RESULTS
In the following, we evaluate the beam-aware DRX and conventional NR DRX mechanism in MATLAB programs. The details of simulation setup and DRX parameter settings

are shown in §VIII-A. We validate the analytical model with the simulation experiments for the beam-aware DRX in §VIII-B with the MATLAB programs. Then, we compare the performance of the beam-aware DRX design and NR DRX mechanism under various parameter settings, including DRX configuration and beam number, in §VIII-C.

A. SIMULATION METHODOLOGY
In the simulation, a gNB has multiple beams to schedule data, and the range of total beam number is from four beams to 20 beams. Also, there are two UEs with omnidirectional antennas camping on each beam. For the beam frame configuration, the length of a beam period (T_b) equals one slot length. We adopt the fourth numerology in the 3GPP NR frame structure, so the slot length is 0.125 *ms* in this paper [54]. Therefore, the length of the serving beam cycle (T_{sbc}^s) varies from 0.5 *ms* to 2.5 *ms*. Like the assumption in §VII, the extremely high data rate in the mmWave band makes the transmission time short enough to be ignored. The packet arrival process is a Poisson distribution with $\lambda = 0.03$ ms^{-1} for each UE. As for the DRX configuration, the DRX parameters in the simulation are picked from the suggested parameters in 3GPP specification [20]. The range of the maximal length of *Inactive* is from 20 *ms* to 100 *ms*, and the DRX cycle length varies from 80 *ms* to 440 *ms*. As we mentioned in §VI, *Inactive* in the beam-aware DRX scheme corresponds to *drx-Inactivity Timer* in the NR DRX. Once receiving any packet arrivals, a UE enters *Active* first and then moves to *Inactive* when there is no incoming packet. We would call the length of one *Active* and N_{ic}^S *Inactive* as "the length of Inactivity Timer" for the readability. In our MATLAB simulation, we use the thermal model in §VII-B to model the UEs' temperatures. The UE's temperature is calculated with equation (8) and equation (9) based on whether the UE's RF module is turned on or turned off. For this thermal model, the time constant (τ) matching the experimental results in [55] is 7.5×10^5 *ms*. We set the environmental temperature (K_{env}) and the highest temperature of the RF module (K_{RF}) as $25°C$ and $45°C$, respectively. In the following experiments, we set the parameters to the default parameter setting in Table 2 if the parameter values are not specified.

B. ANALYTICAL MODEL VERIFICATION
In Figure 9 and Figure 10, we change the length of the DRX cycle and the maximal number of *Inactive* to examine the effects from these DRX parameters and verify the correctness in the analytical model with simulation results. Figure 9(a) depicts that the sleep ratio increases with the long DRX cycle length. Longer DRX cycle length implies longer sleep time in *DRX$_{sleep}$*, so the UE with the longer DRX cycle could

$$P_{ext,n}^S = \begin{cases} e^{-\lambda(N_{ic}^S + 1)T_{sbc}^s}, & \text{when } n = 0 \\ \sum_{f=1}^{min\{n, N_{ic}^S + 1\}} e^{-\lambda T_{sbc}^s(f-1)}(1 - e^{-\lambda T_{sbc}^s}) \cdot P_{ext,n-f}^S, & \text{otherwise} \end{cases} \qquad (21)$$

**TABLE 2.** Default parameter setting for the beam-aware DRX evaluation.

Symbols	The meaning of the symbol	Default value
N	Total beam number of one gNB	8
M_i	Total UE number on beam i $\forall i \in \{1, 2, \cdots, N\}$	2
λ	Inter-arrival rate of each UE	$0.03\ ms^{-1}$
	The length of Inactivity Timer	$61\ ms$ [20]
	The length of DRX cycle	$440\ ms$ [20]
T_{sbc}^s	The length of one serving beam cycle	$1\ ms$
T_b	The length of one beam period	$0.125\ ms$ [54]
τ	The time constant of each UE	$7 \times 10^5\ ms$ [55]
K_{env}	The environmental temperature	$25°C$ [55]
K_{RF}	The highest temperature of the RF module	$45°C$

sleep for a longer duration. With the longer DRX cycle, the UE could save more power; however, the packet delay also increases as Figure 9(b) shows. The packets arriving at the UE in the long sleep time are buffered and yield more severe delay. In Figure 9(c), the UE's steady temperature decreases when the length of the DRX cycle becomes longer. When the wake-up time is fixed, the UE's RF module with a longer DRX cycle would be turned off for a long time, so the steady temperature is lower than that under the configuration with a shorter DRX cycle.

Figure 10(a) demonstrates that the sleep ratio decreases when the length of Inactivity Timer becomes longer. The UE's power consumption in *Active* and *Inactive* is higher than that in *DRX_sleep* and *DRX_check*. The UE with the higher N_{ic}^S is easy to stay in *Active* and *Inactive*, so the sleep ratio is low. The delay of the packet arriving in *Active* and *Inactive* is lower than that in *DRX_sleep* as well. Therefore, the longer the length of Inactivity Timer is, the lower the packet delay is in Figure 10(b). With the higher N_{ic}^S, the probability of the UE entering *Active* and *Inactive* increases. The temperature of UEs in *Active* and *Inactive* is higher than that in *DRX_sleep* because the sleep time in *Active* and *Inactive* is shorter than that in *DRX_sleep*. Thus, in Figure 10(c), the longer length of Inactivity Timer results in a higher steady temperature. Obviously, the longer DRX cycle and the shorter Inactivity Timer result in a higher sleep ratio, a longer packet delay, and a lower steady temperature. By sacrificing the packet delay performance, we could improve both the sleep ratio and the steady temperature under the configuration with the long DRX cycle and the short Inactivity Timer. There is a tradeoff between power efficiency and packet delivery delay; we could enhance one of them according to the requirements in the communication scenarios.
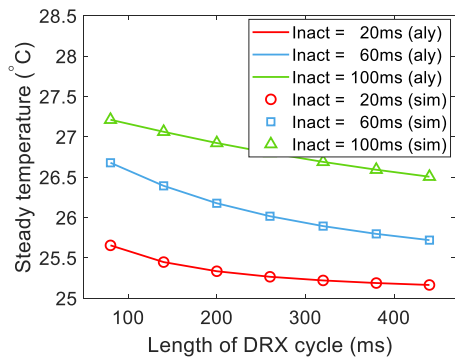
C. COMPARISON WITH OTHER DRX MECHANISM

In the following, we compare the performance of the beam-aware DRX design with that under the 5G NR DRX
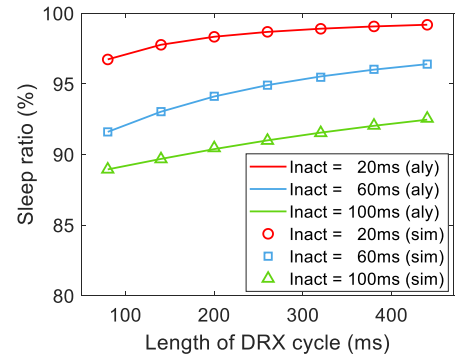
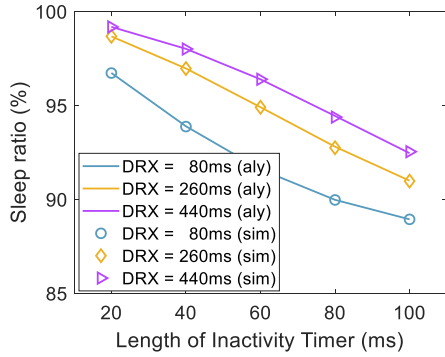(a) Sleep ratio with different N_{dc}^S and N_{ic}^S.
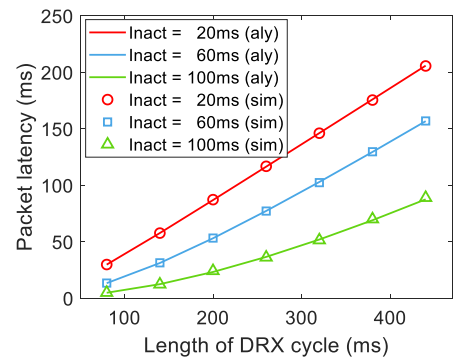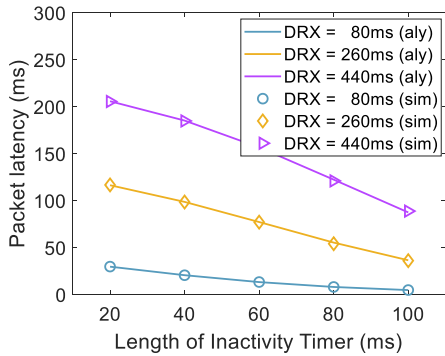

(b) Packet delay with different N_{dc}^S and N_{ic}^S.

(c) Steady temperature with different N_{dc}^S and N_{ic}^S

FIGURE 9. The simulation and analytical results for the beam-aware DRX, where Inact presents the length of Inactivity Timer.

operation in §II-C under the different parameter settings, including the DRX cycle length, the length of Inactivity Timer, and the total beam number of the gNB. We implement the NR DRX mechanisms according to [21] where the UEs control their RF modules based on the NR DRX timers. After the beam management procedure, the gNB knows the UEs' direction and could schedule the PDCCH on the correct beam during each UE's ON Duration. That is, the gNB would choose the correct beam to schedule data when the corresponding UEs wake up. The length of *drx-Inactivity Timer* in the NR DRX corresponds to the duration of one *Active* (T_{sbc}^s) and the maximal period in *Inactive* ($N_{ic}^S \cdot T_{sbc}^s$) in the beam-aware DRX mechanism. In this paper, both of them are referred to as "the length of Inactivity Timer". In the

(a) Sleep ratio with different N_{dc}^S and N_{ic}^S.

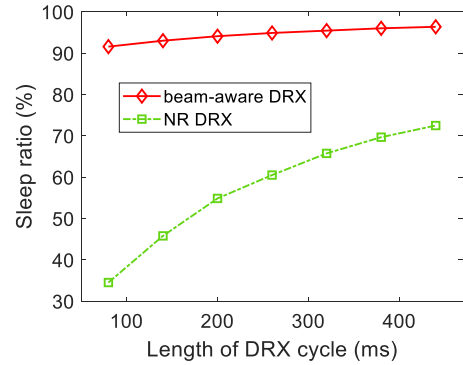(b) Packet delay with different N_{dc}^S and N_{ic}^S.
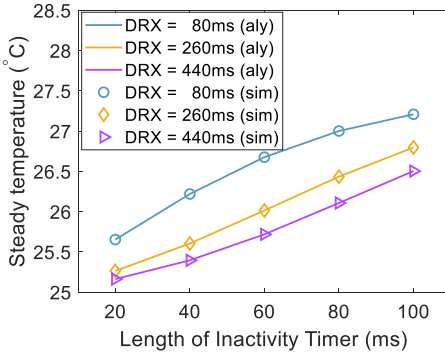
(c) Steady temperature with different N_{dc}^S and N_{ic}^S.

FIGURE 10. The simulation and analytical results for the beam-aware DRX, where DRX presents the length of DRX cycle.

(a) Sleep ratio with different length of DRX cycle.

(b) Packet delay with different length of DRX cycle.
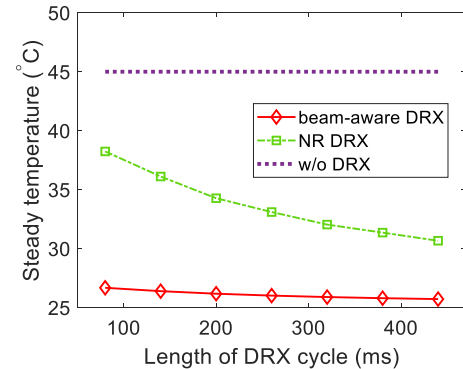
(c) Steady temperature with different length of DRX cycle.

FIGURE 11. Performance results for the beam-aware DRX and 5G NR DRX mechanism with different DRX cycle length.
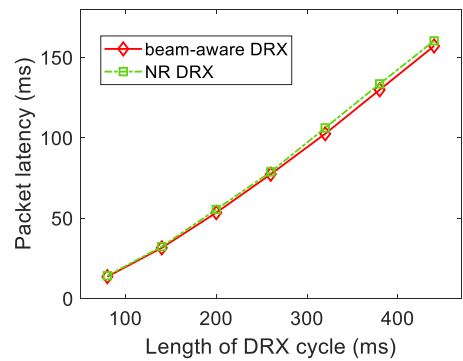
following, we set the length of *drx-Inactivity Timer* in the NR DRX as $N_{ic}^S \cdot T_{sbc}^s + T_{sbc}^s$ ms. Besides, we would adjust the DRX configuration and the beam number of gNB to evaluate the performance of the NR DRX and that of the beam-aware DRX mechanism.

1) EFFECT OF DRX CYCLE
In Figure 11, we would like to compare these two DRX schemes' the performance under different DRX cycle lengths. For the beam-aware DRX mechanism, we set the maximal number of *Inactive* as 60. Since the length of the serving beam cycle is 1 *ms*, the length of Inactivity Timer is 61 *ms* for both the DRX scheme and the NR DRX mechanism. In Figure 11(a) and Figure 11(b), compared with the NR

DRX, the beam-aware DRX could improve the energy efficiency without yielding a more considerable delay. Under the heavy traffic load ($\lambda = 0.03 \ ms^{-1}$), the UEs with both DRX mechanisms are easy to stay in *Active*. With the beam-aware DRX, the UE could only turn on its RF module when the gNB is serving it in *Active* and *Inactive*, so the sleep ratio achieves more than 90%. Besides, the packet delay is mainly ascribed to the DRX cycle, so the delay of these two DRX schemes is similar under the same DRX configuration. Obviously, the beam-aware design could effectively reduce the unnecessary power consumption mentioned in [18] effectively in mmWave communication systems. In Figure 11(c), the steady
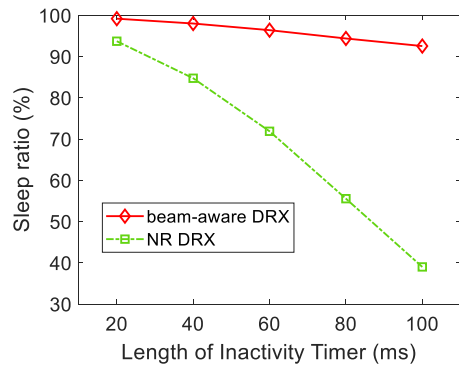
(a) Sleep ratio with different length of Inactivity Timer.
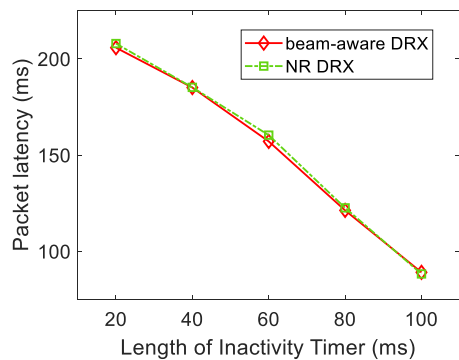
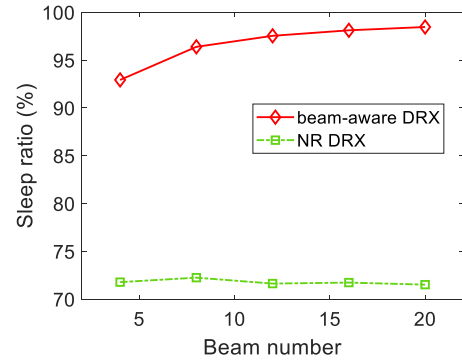(b) Packet delay with different length of Inactivity Timer.
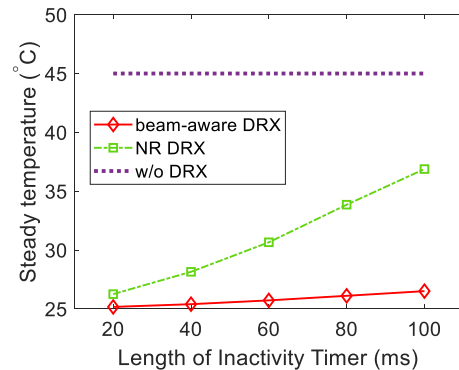
(c) Steady temperature with different length of Inactivity Timer.

FIGURE 12. Performance results for the beam-aware DRX and 5G NR DRX mechanism with different length of Inactivity Timer.

(a) Sleep ratio with different beam number.

(b) Packet delay with different beam number.

(c) Steady temperature with different beam number.

FIGURE 13. Performance results for the beam-aware DRX and 5G NR DRX mechanism with different beam number.
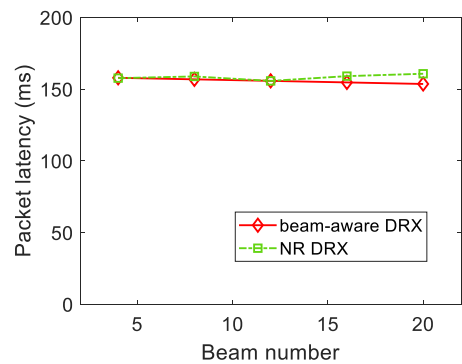
temperature in the NR DRX is much higher than that in the beam-aware DRX mechanism. In the NR DRX, the UE's temperature is even higher than the body temperature when the DRX cycle length is 80 *ms*. In the mmWave communication networks, the heat generated from RF modules is more severe than that in the 4G system. Besides, the high temperature is unacceptable for electronic devices or wearable devices. Thus, the thermal-based design in the DRX mechanism is essential for the mobile device.
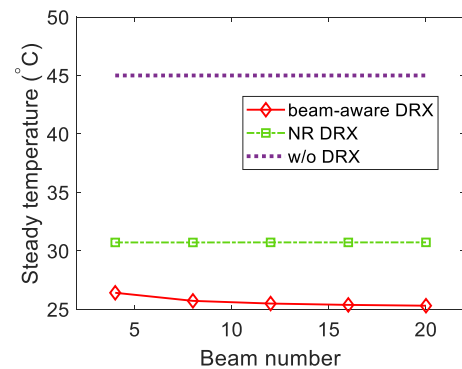
2) EFFECT OF INACTIVITY TIMER
In either the beam-aware DRX mechanism or the NR DRX, we fix the DRX cycle length to 440 *ms* and evaluate the

performance with the different length of Inactivity Timer in Fig. 12. Figure 12(a) depicts that the sleep ratio in beam-aware DRX is much higher than that in NR DRX. According to the serving beam patterns, the UE could properly control its RF module in *Active* and *Inactive*. Thus, the UE would go to sleep to save more power when the gNB uses another beam to serve. In Figure 12(b), the packet delay in the beam-aware DRX and NR DRX is almost the same because we use the same DRX configuration to evaluate the performance. Figure 12(c) shows that the temperature of UE with NR DRX increases massively when the length of Inactivity Timer becomes longer. With the NR DRX, the UE extends its *ON Duration* continuously to receive data; however, it with the beam-aware DRX is only turned on for a

short period many times. Therefore, the UE's temperature in the beam-aware DRX could be reduced effectively with the thermal-based cross-layer design, which is consistent with the observation in §IV.

3) EFFECT OF BEAM NUMBER

The total number of beams for the gNB varies from 4 to 20 in Figure 13. For the DRX configuration, we set the length of Inactivity Timer and that of DRX cycle as 61 *ms* and 440 *ms*, respectively. The beam number has little impact on the performance of NR DRX because the UE operates the NR DRX mechanism according to the packet arrivals instead of serving beam patterns. Therefore, the performance metrics of NR DRX are almost the same under different beam numbers. Figure 13(a) depicts that the sleep ratio in the beam-aware DRX scheme becomes higher when the beam number increases. The UE with the beam-aware DRX goes to sleep when the gNB serves other UEs on the different beams, so the sleep time in one serving beam cycle is longer when the beam number increases. The sleep ratio increases as well. Since we fix the length of Inactivity Timer and that of the DRX cycle, the packet delay of both DRX mechanisms in Figure 13(b) is the same under different beam numbers. In Figure 13(c), the larger the beam number is, the lower the UE's steady temperature is in the beam-aware DRX mechanism. The serving time of the gNB is fixed to one beam period (T_b). In *Active* and *Inactive*, the long sleep time of UE results in the low temperature. Therefore, the performance of the beam-aware DRX surpasses that in NR DRX. Besides, under the mmWave networks with higher beam numbers, the UE operating a beam-aware DRX could save more power and reduce the temperature.

IX. CONCLUSION

5G wireless communications widely applied the beamforming technology to satisfy the high requirements, especially for mmWave communications. The heat generated by the beamforming antenna arrays and RF modules makes the UE overheating issue more vital. The high temperature might damage the function of electronic devices. Besides, beamforming brings the directionality issue to wireless communication links. Such link directionality makes the existing DRX inefficient and wastes precious energy. It is easy for a UE to be "out-of-beam-coverage" in its *ON Duration* when the gNB uses another beam to schedule data.

In this work, we proposed to employ the DRX framework with a beam-aware design to solve UE power consumption and overheating. We use a semi-Markov chain to model the behavior of UEs and validate the model by simulations. Under the heavy traffic load, a beam-aware cross-layer DRX with various DRX cycles provides up to 165.3% improvement in the sleep ratio without a more considerable packet delay. Besides, the UE's temperature under a beam-aware DRX operation decreases from 38.2°C to 26.7°C
as well.

APPENDIX A
TRADITIONAL DRX PERFORMANCE METRICS

According to the semi-Markov model in Figure 5, we could analyze the conventional performance metrics, such as sleep ratio and packet delay, for the beam-aware DRX mechanism in the following.

A. STEADY STATE PROBABILITY

We could use the transition probabilities in §VII-A to derive the steady state probabilities $\Pi^S(m)$ $\forall m \in \mathcal{S}^\mathcal{S}$ for each UE. $\Pi^S(m)$ is the convergent probability distribution over state $S^S m$ for each UE after a massive number of iterations. The steady state probability matrix is

$$\Pi^{\mathbf{S}} = \begin{bmatrix} \Pi^S(1) & \Pi^S(2_1) & \dots & \Pi^S(2_{N_{ic}^B}) & \Pi^S(3) & \Pi^S(4) \end{bmatrix}.$$

We could calculate $\Pi^{\mathbf{S}}$ via the following global balance equation.

$$\begin{cases} \Pi^{\mathbf{S}} \cdot \mathbf{P}^{\mathbf{S}} = \Pi^{\mathbf{S}} \\ \Pi^{\mathbf{S}} \cdot \mathbf{J}_{|\mathcal{S}^\mathcal{S}|,\mathbf{1}} = 1, \end{cases} \qquad (23)$$

where $\mathbf{J}_{\mathbf{x},\mathbf{y}}$ is a *x*-by-*y* matrix with all its entries equal to one.

Despite the steady state probabilities, we need the expected holding time ($\mathsf{E}\{T_h^S(m)\}$ $\forall m \in \mathcal{S}^\mathcal{S}$) in each state to derive the performance metrics in the beam-aware DRX. Figure 4 shows that the holding time in *Active* and *Inactive* is

$$\mathsf{E}\{T_h^S(1)\} = \mathsf{E}\{T_h^S(2_m)\} = T_{sbc}^s \quad \forall m \in \{1, 2, \dots, N_{ic}^S\}. \quad (24)$$

Also, the DRX cycle length is $N_{dc}^B \cdot T_{sbc}^s$. The UEs will turn on their RF module for one beam period at the end of each DRX cycle to check whether there are any buffered packets or not. Therefore, we could express the expected holding time in *DRX_check* and *DRX_sleep* as

$$\mathsf{E}\{T_h^S(3)\} = T_b \qquad (25)$$
$$\mathsf{E}\{T_h^S(4)\} = N_{dc}^S T_{sbc}^s - T_b. \qquad (26)$$

B. SLEEP RATIO

Sleep ratio (R^S) and packet delay (D^S) are the two main performance metrics of the DRX mechanism. For each UE, R^S is the ratio of accumulated sleeping duration to the total observed time. A UE with a higher R^S means that it consumes less power during the observed time. We could use the steady state probability ($\Pi^S(m)$ $\forall m \in \mathcal{S}^\mathcal{S}$) and the expected holding time ($\mathsf{E}\{T_h^S(m)\}$ $\forall m \in \mathcal{S}^\mathcal{S}$) to express $\mathsf{E}\{R^S\}$ as

$$\mathsf{E}\{R^S\}$$
$$= \frac{\sum_{m \in \mathcal{S}^\mathcal{S} \backslash \{3,4\}} \Pi^S(m)(T_{sbc}^s - T_b) + \Pi^S(4)\mathsf{E}\{T_h^S(4)\}}{\sum_{m \in \mathcal{S}^\mathcal{S}} \Pi^S(m) \cdot \mathsf{E}\{T_h^S(m)\}}.$$
$$(27)$$

C. PACKET DELAY

A gNB would buffer the packets arriving at the sleeping UE, and then the packet delay (D^S) increases. D^S is the period from the time when a packet arrives in the gNB's buffer to the time when the corresponding UE receives it. In this paper,

we assume the best beam pairs are already established, so the packet delay does not contain the delay caused by the beam searching process. We need to calculate the expected delay in each state firstly to get the overall packet delay. The delay is caused by both the beam pattern in *Active* and *Inactive* and the long sleep time in DRX_{sleep}. The expected delay of active UEs is

$$d_{act}^S = \frac{1}{2T_{sbc}^s}(T_{sbc}^s - T_b)^2. \tag{28}$$

Besides, the expected delay of a packet buffered in UEs' sleep time could be expressed as

$$d_{sleep}^S = \frac{1}{2}(N_{dc}^S T_{sbc}^s - T_b). \tag{29}$$

Since the overall average delay contains the weighted summation of the expected delay in each state, we derive the expected overall packet delay as

$$\mathsf{E}\{D^S\} = \frac{1}{\sum_{m \in \mathcal{S}^S} \Pi^S(m) \cdot \mathsf{E}\{T_h^S(m)\}}$$
$$\cdot \left[\sum_{m \in \mathcal{S}^S \setminus \{3,4\}} \Pi^S(m) \mathsf{E}\{T_h^S(m)\} d_{act}^S \right.$$
$$\left. + \Pi^S(4) \mathsf{E}\{T_h^S(4)\} d_{sleep}^S \right]. \tag{30}$$

REFERENCES

[1] A. Ghosh, T. A. Thomas, M. C. Cudak, R. Ratasuk, P. Moorut, F. W. Vook, T. S. Rappaport, G. R. MacCartney, S. Sun, and S. Nie, "Millimeter-wave enhanced local area systems: A high-data-rate approach for future wireless networks," *IEEE J. Sel. Areas Commun.*, vol. 32, no. 6, pp. 1152–1163, Jun. 2014.

[2] S. Rangan, T. S. Rappaport, and E. Erkip, "Millimeter-wave cellular wireless networks: Potentials and challenges," *Proc. IEEE*, vol. 102, no. 3, pp. 366–385, Mar. 2014.

[3] S. Sur, I. Pefkianakis, X. Zhang, and K.-H. Kim, "Towards scalable and ubiquitous millimeter-wave wireless networks," in *Proc. 24th Annu. Int. Conf. Mobile Comput. Netw.*, Oct. 2018, pp. 257–271.

[4] A. Thornburg, T. Bai, and R. W. Heath, Jr., "Interference statistics in a random mmWave ad hoc network," in *Proc. IEEE Int. Conf. Acoust., Speech Signal Process. (ICASSP)*, Apr. 2015, pp. 2904–2908.

[5] H. Shokri-Ghadikolaei, C. Fischione, G. Fodor, P. Popovski, and M. Zorzi, "Millimeter wave cellular networks: A MAC layer perspective," *IEEE Trans. Commun.*, vol. 63, no. 10, pp. 3437–3458, Oct. 2015.

[6] R. W. Heath, Jr., "Millimeter wave: The future of commercial wireless systems," in *Proc. IEEE Compound Semiconductor Integr. Circuit Symp. (CSICS)*, Oct. 2016, pp. 1–4.

[7] F. Sohrabi and W. Yu, "Hybrid digital and analog beamforming design for large-scale antenna arrays," *IEEE J. Sel. Topics Signal Process.*, vol. 10, no. 3, pp. 501–513, Apr. 2016.

[8] B. Park, S. Jin, D. Jeong, J. Kim, Y. Cho, K. Moon, and B. Kim, "Highly linear mm-wave CMOS power amplifier," *IEEE Trans. Microw. Theory Techn.*, vol. 64, no. 12, pp. 4535–4544, Dec. 2016.

[9] A. Maltsev, A. Sadri, A. Pudeyev, and I. Bolotin, "Highly directional steerable antennas: High-gain antennas supporting user mobility or beam switching for reconfigurable backhauling," *IEEE Veh. Technol. Mag.*, vol. 11, no. 1, pp. 32–39, Mar. 2016.

[10] A. V. Lopez, A. Chervyakov, G. Chance, S. Verma, and Y. Tang, "Opportunities and challenges of mmWave NR," *IEEE Wireless Commun.*, vol. 26, no. 2, pp. 4–6, Apr. 2019.

[11] Qualcomm. (2019). *Breaking the Wireless Barriers to Mobilize 5G NR mmWave*. [Online]. Available: https://www.qualcomm.com/documents/webinar-breaking-wireless-barriers-mobilize-5g-nr-mmwave

[12] T. Starner, "How wearables worked their way into the mainstream," *IEEE Pervasive Comput.*, vol. 13, no. 4, pp. 10–15, Oct./Dec. 2014.

[13] K. Venugopal, M. C. Valenti, and R. W. Heath, Jr., "Device-to-device millimeter wave communications: Interference, coverage, rate, and finite topologies," *IEEE Trans. Wireless Commun.*, vol. 15, no. 9, pp. 6175–6188, Sep. 2016.

[14] *Study on User Equipment (UE) Power Saving in NR*, document TR 38.840, 3GPP, Version 16.0.0, 2019.

[15] C.-H. Ho, A. Huang, P.-J. Hsieh, and H.-Y. Wei, "Energy-efficient millimeter-wave M2M 5G systems with beam-aware DRX mechanism," in *Proc. IEEE 86th Veh. Technol. Conf. (VTC-Fall)*, Sep. 2017, pp. 1–5.

[16] C.-W. Weng, K.-H. Lin, B. P. S. Sahoo, and H.-Y. Wei, "Beam-aware dormant and scheduling mechanism for 5G millimeter wave cellular systems," *IEEE Trans. Veh. Technol.*, vol. 67, no. 11, pp. 10935–10949, Nov. 2018.

[17] C.-W. Weng, B. P. S. Sahoo, C.-C. Chou, and H.-Y. Wei, "Efficient beam sweeping paging in millimeter wave 5G networks," in *Proc. IEEE Int. Conf. Commun. Workshops (ICC Workshops)*, May 2018, pp. 1–6.

[18] A. Huang, K.-H. Lin, and H.-Y. Wei, "Beam-aware cross-layer DRX design for 5G millimeter wave communication system," *IEEE Access*, vol. 8, pp. 77604–77617, 2020.

[19] *NR; Overall Description; Stage-2*, document TS 38.300, 3GPP, Version 16.1.0, Apr. 2020.

[20] *NR; Radio Resource Control (RRC); Protocol Specification*, document TS 38.331, 3GPP, Version 16.1.0, 2020.

[21] *NR; Medium Access Control (MAC) Protocol Specification*, document TS 38.321, 3GPP, Version 16.3.0, Jan. 2021.

[22] G. Pocovi, I. Thibault, T. Kolding, M. Lauridsen, R. Canolli, N. Edwards, and D. Lister, "On the suitability of LTE air interface for reliable low-latency applications," in *Proc. IEEE Wireless Commun. Netw. Conf. (WCNC)*, Apr. 2019, pp. 1–6.

[23] H.-W. Ferng, Y.-T. Tseng, and T.-H. Wang, "Parameter-adaptive dynamic and adjustable DRX schemes for LTE/LTE-A," *IEEE Trans. Green Commun. Netw.*, vol. 3, no. 4, pp. 1035–1043, Dec. 2019.

[24] X.-N. Fan, Q.-S. Hu, and G.-J. Cao, "Grouping-based extended discontinuous reception with adjustable eDRX cycles for smart grid," in *Proc. IEEE Int. Conf. Commun., Control, Comput. Technol. Smart Grids (SmartGridComm)*, Oct. 2019, pp. 1–5.

[25] B. Cai, Y. Chen, and I. Darwazeh, "Analyzing energy efficiency for IoT devices with DRX capability and Poisson arrivals," in *Proc. 26th Int. Conf. Telecommun. (ICT)*, Apr. 2019, pp. 254–259.

[26] A. Bin-Salem, S. Bindahman, S. M. Hanshi, W. Munassar, and K. Aladhal, "Efficient power-delay management framework for enhancing the lifetime of IoT devices," in *Proc. 1st Int. Conf. Intell. Comput. Eng. (ICOICE)*, Dec. 2019, pp. 1–5.

[27] F. Moradi, E. Fitzgerald, and B. Landfeldt, "Modeling DRX for D2D communication," *IEEE Internet Things J.*, vol. 8, no. 4, pp. 2574–2584, Feb. 2021.

[28] D. Selvamuthu, R. Raj, K. Sahu, and A. Aggarwal, "Energy harvesting modelling and analysis in LTE-A networks with DRX scheme," in *Proc. IEEE Globecom Workshops (GC Wkshps)*, Dec. 2019, pp. 1–6.

[29] D. S. Roy, "A study on DRX mechanism for wireless powered LTE-enabled IoT devices," in *Proc. IEEE Int. Conf. Consum. Electron., Taiwan (ICCE-TW)*, May 2019, pp. 1–2.

[30] M. Lauridsen, G. Berardinelli, F. M. L. Tavares, F. Frederiksen, and P. Mogensen, "Sleep modes for enhanced battery life of 5G mobile terminals," in *Proc. IEEE 83rd Veh. Technol. Conf. (VTC Spring)*, May 2016, pp. 1–6.

[31] A. Khlass, D. Laselva, and R. Jarvela, "On the flexible and performance-enhanced radio resource control for 5G NR networks," in *Proc. IEEE 90th Veh. Technol. Conf. (VTC-Fall)*, Sep. 2019, pp. 1–6.

[32] M. Lauridsen, D. Laselva, F. Frederiksen, and J. Kaikkonen, "5G new radio user equipment power modeling and potential energy savings," in *Proc. IEEE 90th Veh. Technol. Conf. (VTC-Fall)*, Sep. 2019, pp. 1–6.

[33] S. Rostami, K. Heiska, O. Puchko, K. Leppanen, and M. Valkama, "Pre-grant signaling for energy-efficient 5G and beyond mobile devices: Method and analysis," *IEEE Trans. Green Commun. Netw.*, vol. 3, no. 2, pp. 418–432, Jun. 2019.

[34] S. Rostami, H. D. Trinh, S. Lagen, M. Costa, M. Valkama, and P. Dini, "Wake-up scheduling for energy-efficient mobile devices," *IEEE Trans. Wireless Commun.*, vol. 19, no. 9, pp. 6020–6036, Sep. 2020.

[35] S. Rostami, S. Lagen, M. Costa, M. Valkama, and P. Dini, "Wake-up radio based access in 5G under delay constraints: Modeling and optimization," *IEEE Trans. Commun.*, vol. 68, no. 2, pp. 1044–1057, Feb. 2020.

[36] S. Rostami, K. Heiska, O. Puchko, K. Leppanen, and M. Valkama, "Novel wake-up scheme for energy-efficient low-latency mobile devices in 5G networks," *IEEE Trans. Mobile Comput.*, early access, Jan. 6, 2020, doi: 10.1109/TMC.2020.2964218.

[37] S. Rostami, S. Lagen, M. Costa, P. Dini, and M. Valkama, "Optimized wake-up scheme with bounded delay for energy-efficient MTC," in *Proc. IEEE Global Commun. Conf. (GLOBECOM)*, Dec. 2019, pp. 1–6.

[38] S. H. A. Shah, S. Aditya, S. Dutta, C. Slezak, and S. Rangan, "Power efficient discontinuous reception in THz and mmWave wireless systems," in *Proc. IEEE 20th Int. Workshop Signal Process. Adv. Wireless Commun. (SPAWC)*, Jul. 2019, pp. 1–5.

[39] L. Sharma, B. B. Kumar, and S.-L. Wu, "Performance analysis and adaptive DRX scheme for dual connectivity," *IEEE Internet Things J.*, vol. 6, no. 6, pp. 10289–10304, Dec. 2019.

[40] Z. Zhang, Q. Zhu, and P. Zhang, "Fast beam tracking discontinuous reception for D2D-based UAV mmWave communication," *IEEE Access*, vol. 7, pp. 110487–110498, 2019.

[41] M. K. Maheshwari, M. Agiwal, N. Saxena, and A. Roy, "Directional discontinuous reception (DDRX) for mmWave enabled 5G communications," *IEEE Trans. Mobile Comput.*, vol. 18, no. 10, pp. 2330–2343, Oct. 2019.

[42] M. Agiwal, M. K. Maheshwari, N. Saxena, and A. Roy, "Directional-DRX for 5G wireless communications," *Electron. Lett.*, vol. 52, no. 21, pp. 1816–1818, Oct. 2016.

[43] M. K. Maheshwari, M. Agiwal, N. Saxena, and A. Roy, "Hybrid directional discontinuous reception (HD-DRX) for 5G communication," *IEEE Commun. Lett.*, vol. 21, no. 6, pp. 1421–1424, Jun. 2017.

[44] D. Liu, C. Wang, and L. K. Rasmussen, "Discontinuous reception for multiple-beam communication," *IEEE Access*, vol. 7, pp. 46931–46946, 2019.

[45] M. K. Maheshwari, A. Roy, and N. Saxena, "Analytical modeling of DRX with flexible TTI for 5G communications," *Trans. Emerg. Telecommun. Technol.*, vol. 29, no. 2, p. e3275, Feb. 2018.

[46] N. R. Philip and B. Malarkodi, "Extended hybrid directional DRX with auxiliary active cycles for light traffic in 5G networks," *Trans. Emerg. Telecommun. Technol.*, vol. 30, no. 1, p. e3552, Jan. 2019.

[47] A. K. Singh, S. Dey, K. McDonald-Maier, K. R. Basireddy, G. V. Merrett, and B. M. Al-Hashimi, "Dynamic energy and thermal management of multi-core mobile platforms: A survey," *IEEE Des. Test*, vol. 37, no. 5, pp. 25–33, Oct. 2020.

[48] G. Singla, G. Kaur, A. K. Unver, and U. Y. Ogras, "Predictive dynamic thermal and power management for heterogeneous mobile platforms," in *Proc. Design, Automat. Test Eur. Conf. Exhib. (DATE)*, 2015, pp. 960–965.

[49] A. Prakash, H. Amrouch, M. Shafique, T. Mitra, and J. Henkel, "Improving mobile gaming performance through cooperative CPU-GPU thermal management," in *Proc. 53rd ACM/EDAC/IEEE Annu. Design Automat. Conf. (DAC)*, Jun. 2016, pp. 1–6.

[50] O. Sahin and A. K. Coskun, "On the impacts of greedy thermal management in mobile devices," *IEEE Embedded Syst. Lett.*, vol. 7, no. 2, pp. 55–58, Jun. 2015.

[51] F. L. Tan and C. P. Tso, "Cooling of mobile electronic devices using phase change materials," *Appl. Thermal Eng.*, vol. 24, no. 2, pp. 159–169, Feb. 2004.

[52] M. Giordani, M. Polese, A. Roy, D. Castor, and M. Zorzi, "A tutorial on beam management for 3GPP NR at mmWave frequencies," *IEEE Commun. Surveys Tuts.*, vol. 21, no. 1, pp. 173–196, 1st Quart., 2019.

[53] W. M. Rohsenow, J. P. Hartnett, and Y. I. Cho, *Handbook of Heat Transfer*, vol. 3. New York, NY, USA: McGraw-Hill, 1998.

[54] *NR; Physical Channels and Modulation*, document TS 38.211, 3GPP, Version 16.1.0, 2020.

[55] Q. Xie, J. Kim, Y. Wang, D. Shin, N. Chang, and M. Pedram, "Dynamic thermal management in mobile devices considering the thermal coupling between battery and application processor," in *Proc. IEEE/ACM Int. Conf. Comput.-Aided Design (ICCAD)*, Nov. 2013, pp. 242–247.

AN HUANG (Student Member, IEEE) received the B.S. degree in electrical engineering from National Taiwan University, Taipei, Taiwan, in 2018, where she is currently pursuing the M.S. degree in communication engineering. She was a summer intern with Foxconn, in 2017. Since 2016, she has been working on DRX projects with the Wireless and Mobile Networking Laboratory led by Prof. H.-Y. Wei.

KUANG-HSUN LIN (Graduate Student Member, IEEE) received the B.S. degree in electrical engineering degree from National Taiwan University, Taipei, Taiwan, in 2015, where he is currently pursuing the Ph.D. degree in communication engineering with the Graduate Institute of Communication Engineering (GICE). He held summer internships with MediaTek from Summer 2015 to 2018. Since 2015, he has been working with the Wireless Mobile Networking Laboratory led by Prof. H.-Y. Wei.

HUNG-YU WEI (Senior Member, IEEE) received the B.S. degree in electrical engineering from National Taiwan University (NTU), Taipei, Taiwan, in 1999, and the M.S. and Ph.D. degrees in electrical engineering from Columbia University, New York, NY, USA, in 2001 and 2005, respectively.

He was a Summer Intern with Telcordia Applied Research, from 2000 to 2001. From 2003 to 2005, he was with NEC Labs America. He joined the Department of Electrical Engineering, National Taiwan University, in July 2005. He is currently a Professor with the Department of Electrical Engineering and the Graduate Institute of Communication Engineering, National Taiwan University. He actively participates in wireless communications standardization activities. His research interests include broadband wireless communications, vehicular networking, cross-layer design for wireless multimedia communications, the Internet of Things, and game theoretic models for networking. He was a Consulting Member with the Acts and Regulation Committee, National Communications Commission, from 2008 to 2009, and a Voting Member of the IEEE 802.16 working group. He received the Recruiting Outstanding Young Scholar Award from the Foundation for the Advancement of Outstanding Scholarship, in 2006, the K. T. Li Young Researcher Award from the ACM Taipei Chapter and IICM, in 2012, the CIEE Excellent Young Engineer Award, in 2014, and the NTU Excellent Teaching Award, in 2008, the Excellent Young Scholars Award for the Research Project, from the Taiwan's Ministry of Science and Technology, in 2014, and the Wu Ta-You Memorial Award from the Ministry of Science and Technology, in 2015. He served as the Chair for the IEEE Vehicular Technology Society Taipei Chapter. He is the Chair of IEEE P1935 standard working group on Edge/Fog Manageability and Orchestration.

• • •